Domain Structure of Rochelle Salt and KH_2PO_4†

TOSHITO MITSUI AND JIRO FURUICHI
Faculty of Science, Hokkaido University, Sapporo, Japan

(Received January 14, 1952; revised manuscript received December 1, 1952)

It has been verified by means of the polarization microscope that rochelle salt in the ferroelectric state consists of many domains. The domain structure in an annealed crystal is caused by the electrostatic self energy. When the electric field along the X direction is increased and then decreased gradually, successive positions of the domain wall produce a hysteresis loop, which proves the existence of a restoring force on the wall. This restoring force causes lag of charging, and its variation with time produces a fatigue effect. The propagation velocity of a domain wall is about 0.2 cm/sec for 100 v/cm. A group of domains parallel to the b axis has been created artificially. When a stress Y_z is applied, a set of domains inverts its polarization direction. Z-cut specimens of KH_2PO_4 cooled below the Curie temperature divide into many regions which appear to be domains. The phase transition in KH_2PO_4 propagates from only one nucleus.

Theoretically it has been concluded that the domain wall energy of rochelle salt is $1.4\times10^{-10}P_0^3$ erg/cm^2 and the wall width $\sim2\times10^{-4}/P_0$ cm, where P_0 is the saturation polarization.

I. INTRODUCTION

MUCH experimental evidence exists that, in general, ferroelectric crystals consist of many domains.[1] For $BaTiO_3$ this has been proved conclusively by means of the polarization microscope, and the domain structure has been investigated in detail.[2] For rochelle salt and KH_2PO_4 the existence of domain structure has been conclusively demonstrated by x-ray studies,[3] but many details are still lacking. In our work, described below, the domain structure of these two crystals has been examined by means of the polarization microscope, and the properties of the domains in rochelle salt have been investigated both experimentally and theoretically.

II. POSSIBILITY OF OBSERVATION OF DOMAIN STRUCTURE

As has been shown in the investigations of the domain structure of $BaTiO_3$, examination by means of the polarization microscope is the most direct method to investigate the domain structure of ferroelectric crystals. But this method is useful only in those cases in which the directions of the optical axes of a domain differ from those of its neighbors. Rochelle salt outside the Curie region (between 24°C and −18°C) belongs to the orthorhombic symmetry class V; its optical axes a, b, and c are parallel to the c, b, and a axes, respectively; between the two Curie points it polarizes spontaneously along the X direction and its symmetry becomes monoclinic C_2 owing to the spontaneous deformation y_z^0. This means that in a domain the b or the c axis[4] deviates from its original direction in the rhombic crystal and, as one would expect in monoclinic crystals, the a and b axes may deviate from the c and b axes, respectively. While the former deviation is very small as y_z^0 is very small (its maximum value is about 3′), the latter deviation does not necessarily have the same order of magnitude as y_z^0. In addition, the angle between the a or b axes of neighboring domains is twice the deviation angle from the c or b axes (Fig. 1), so

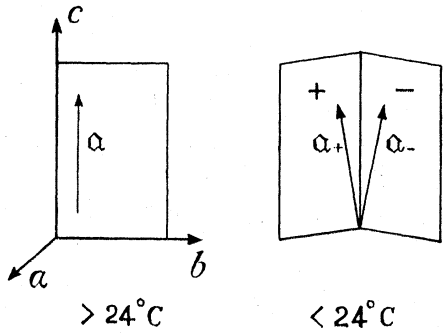

FIG. 1. Deviation of the optical axis a caused by spontaneous deformation in rochelle salt.

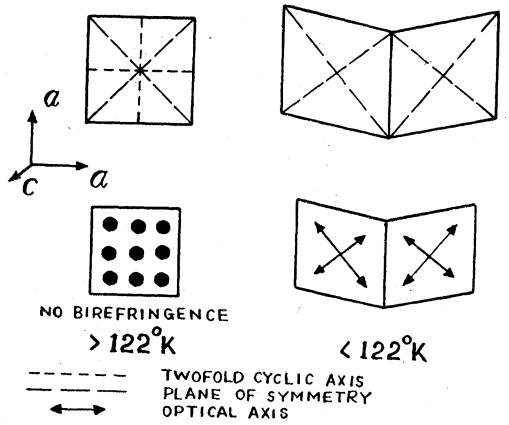

FIG. 2. Symmetry element and double refraction of KH_2PO_4.

† This work was supported in part by the Scientific Research Expenditure and the Scientific Research Subsidy of the Ministry of Education.

[1] For a review of the investigations on rochelle salt and KH_2PO_4, see W. G. Cady, *Piezoelectricity* (McGraw-Hill Book Company, Inc., New York, 1946).

[2] B. Matthias and A. von Hippel, Phys. Rev. **73**, 1378 (1948); P. W. Forsbergh, Jr., Phys. Rev. **76**, 1187 (1949).

[3] S. Miyake, Proc. Phys.-Math. Soc. Japan **23**, 377, 810 (1941); J. Phys. Soc. Japan **2**, 98 (1947); A. R. Ubbelohde and I. Woodward, Proc. Roy. Soc. (London) **A185**, 448 (1946); **188**, 358 (1947).

[4] In this paper the crystallographic axes of domains paralle or almost parallel to the a, b, and c axes of a large pseudorhomic crystal are called a, b, and c, respectively.

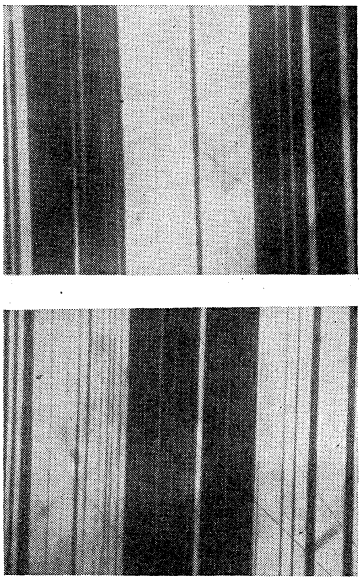

FIG. 3. X-cut specimen of rochelle salt observed between crossed Nicols (×50). The c axis is rotated from the plane of a Nicol (A) to the left; (B) to the right.

that, if the deviation is large enough, the domain structure of an X-cut specimen can be observed between crossed Nicols by the difference of the extinction positions of neighboring domains.

KH_2PO_4 above the Curie point at 122°K belongs to the tetragonal symmetry class V_d, which is optically uniaxial: the c axis is the optic axis. Below the Curie point the crystal polarizes spontaneously along the Z direction and acquires orthorhombic symmetry C_{2v} owing to the spontaneous deformation x_y^0 which is an elongation or contraction along the plane of symmetry (Fig. 2). Hence the crystal becomes optically biaxial and one of its three optical axes is parallel to the c axis, while the other two are parallel to the two planes of symmetry. Hence each of the latter axes of a domain is almost perpendicular to the corresponding axes of neighboring domains, as shown in Fig. 2. This implies that a Z-cut specimen of KH_2PO_4 has no birefringence above the Curie point but a finite birefringence below. Then, if the magnitude of the birefringence is comparatively large, the color of the domains polarized in one sense may be somewhat different from that of the other domains when a Z-cut specimen is put at a 45° position and is observed through a birefringent plate. Besides, if the absorption coefficients along the two axes differ sufficiently from each other, the domain structure may be observed by the different colors in polarized light. Further, since the spontaneous deformation is comparatively large (27′), there is some possibility of observing the domain structure by the difference of the extinction positions of neighboring domains.

III. DOMAIN STRUCTURE OF ROCHELLE SALT

The specimens of rochelle salt were ground down with emergy paper and polished with rouge. Inspection of X-cut specimens between crossed Nicols reveals that in reality they consist of two sets of regions which have slightly different extinction positions. The specimens are divided into many dark and light regions; when the c axes were rotated the light and dark regions were interchanged (Fig. 3). The angle between the two extinction positions is about 2.5° at 17°C. The structure disappears near 23°C and below about −18°C and, as described below, the effects of applying an electric field and mechanical stresses prove that each region itself is a domain. On Y-cut and Z-cut specimens such a pattern was not observed, a fact which is to be expected from the arrangement of the optical axes.

In general, each region appears as a band parallel to the c axis. Specimens cut parallel to the b axis and oblique to the a and c axes show bands perpendicular to the b axis. Consequently, a domain is a slab perpendicular to the b axis. The domain widths which have been observed range from 5×10^{-1} to 1×10^{-4} cm. Most specimens have also groups of domains perpendicular to the c axis (Figs. 4 and 5). Domains parallel to the b axis or c axis, respectively, will be designated as b domains and c domains. Some groups of b domains occupy a rectangular region of which the boundaries are parallel to the b or c axis. Sometimes a group of fine b domains occupies a part of the surface of a specimen, of which the circumference and bottom consist of wider c domains (Fig. 4A). In a few cases the upper half of a a specimen consist of b domains and the lower half of c

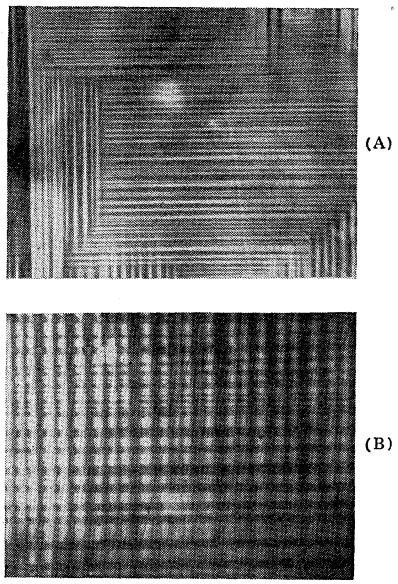

FIG. 4. Co-existence of b and c domains. (A) A group of fine b domains at the crystal surface (×80). (B) A specimen of which the upper half consists of b domains and the lower half c domains (×50).

domains with almost the same widths (Fig. 4B). There are fewer *b* domains than *c* domains, and when the surface is polished *b* domains tend to disappear in favor of *c* domains. This proves that the structure of the *c* domains is more stable than that of the *b* domains. Sometimes annealing causes replacement of the *b* domains by the *c* domains; in other cases there is little effect.

These structures seem to form during the growth of the crystals. Inspection of thin crystals produced in the Kobayashi Institute of Physical Research by restraining their growth along the *X* direction, and not subjected to any treatment, cutting or polishing, show that more groups of *b* domains are found in the part having its surface parallel to the *b* axis during the crystal growth than in those parallel to the *c* axis. The largest single domain crystal, which was 0.5 cm along the *b* axis and 1.0 cm along the *c* axis, was grown by evaporation. Ideal conditions of crystallization may produce large single domain crystals. When a domain terminates within a crystal, it becomes generally wedge-shaped (Figs. 4A and 5). The wedge angle is not always the same but varies usually by several degrees. Some of them are prow-shaped rather than wedge-shaped, i.e., their boundaries are not parallel to the *a* axis (the *b* domains in Fig. 4A).

In crystals glued on glass, in which the internal stresses may be strong, special domain structures have been found (Fig. 5). The figure shows a structure forming around a small hole. Such structures are also observed in rochelle salt crystal containing Cu ions produced by M. Marutake, even if they were not glued on glass.

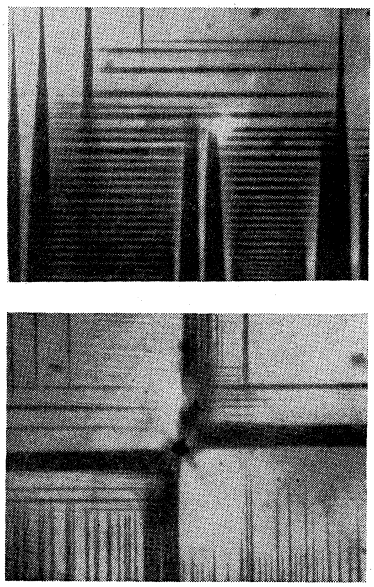

FIG. 5. Domain structure caused by strong internal stress (×80). The *b* and *c* directions are the same as in Fig. 4. (A) Peculiar co-existence of *b* and *c* domains. (B) Domain structure around a hole (black spot in the center).

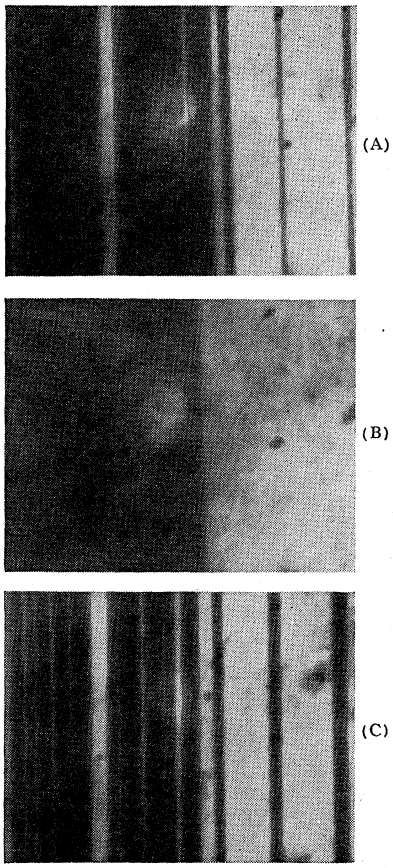

FIG. 6. Effect of temperature (×210). (A) 15°C. (B) 22°C. (C) 15°C after keeping at about 25°C for several minutes.

IV. EFFECT OF TEMPERATURE AND ANNEALING

The domain structure varies with temperature as shown in Figs. 6A and 6B. Some of the wedge-shaped domains evidently become thin and short with increasing temperature and expand again as the temperature is decreased. This may be a consequence of the variation of the internal stresses caused by the variation of the spontaneous deformation.

If crystals are warmed above the Curie point for several minutes and then cooled, the domain structure is similar, but somewhat different from the original one, (Figs. 6A and 6C). A specimen kept at a high temperature for a long time and then cooled to room temperature has a very different domain structure consisting of very fine domains (Figs. 7 and 8). If the annealed crystal is immersed in saturated rochelle salt solution after it is cooled to room temperature, the domain width increases.

Figure 9 shows a correlation between the domain width *W* and its thickness *D*. In one of the eight specimens of regular domain structure, the domain width *W*

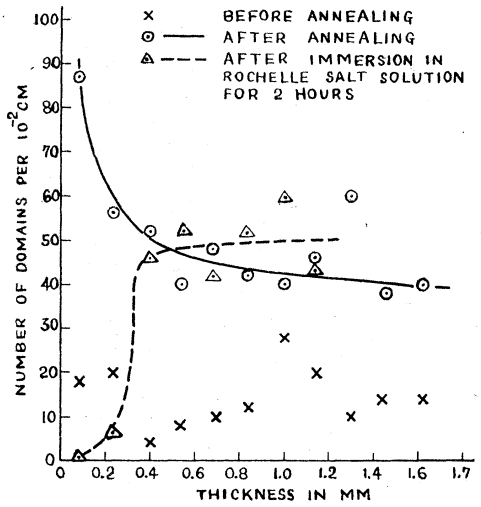

FIG. 7. Effect of annealing and immersion in rochelle salt solution.

was almost perfectly proportional to the square root of the thickness D (Fig. 10). The curve, $W=1.1\times10^{-3}D^{\frac{1}{2}}$, drawn in Fig. 9, represents comparatively well the observed relation for thin crystals.

As is well known, the ferromagnetic domain structure makes the free energy, consisting of magnetic self energy, domain wall, magnetostrictive and anisotropy energy, a minimum. In ferroelectric crystals the electrostatic energy plays no role in general and the internal stresses are a principal factor determining the domain structure, as shown by Forsbergh[2] and also in the present paper (see Sec. V). We might therefore expect that annealing would tend to produce a single domain crystal, but the experimental results reported above indicate that there is some additional factor causing domain formation. If the crystal polarizes more or less abruptly, the electrostatic self energy may contribute to the domain structure unless the surface charge is neutralized immediately. If the domain structure thus formed persists even after the charge is neutralized, a correlation between the domain width and the thickness of the crystal might be expected. In addition, if the wall moves after the neutralization, a charge density $2P_0$ may develop on the (100) surfaces across which the wall has moved; P_0 is the saturation polarization. Thus an electric restoring force on the wall may result. When the specimen, cooled to room temperature, is immersed in an electrolytic solution these charges and thus this restoring force cannot develop, and the displacements of the walls due to their thermal motion may occur more frequently than for the walls in the dry crystal.

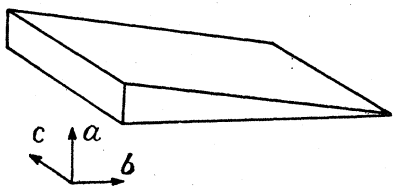

FIG. 8. Specimen to study the effect of annealing.

This may explain the effect of the immersion in rochelle salt solution (Fig. 7).

V. EFFECT OF ELECTRIC FIELD AND INTERNAL FORCE ON THE DOMAIN WALL

The effect of an electric field was observed through a hole in an aluminum foil electrode. At the start of the experiment the hole was covered with an NaCl solution in glycerin which provided a transparent electrode.

When the field is applied, alternate domains expand and contract, respectively. The relation between the sense of the polarization of a domain and the arrangement of the optical axes can be determined by observing which of the two extinction positions those domains possess which expand when the field is applied in one sense. The result is as follows: if we observe a domain facing the surface with positive change, the optical axis a deviates from the c axis to the left (Fig. 1).

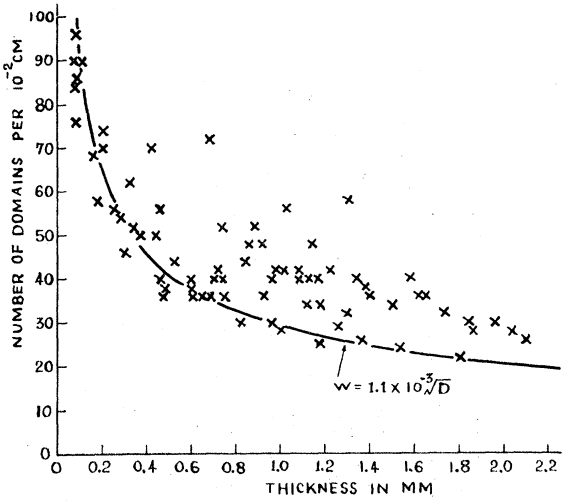

FIG. 9. Number of domains per 10^{-2} cm *vs* thickness.

Inspection under high magnification reveals that the displacement of the domain wall is often discontinuous and that the successive positions of the wall produce a hysteresis loop when the field is increased and then decreased gradually (Fig. 11). The loop suggests that the force on the wall consists of two parts: one is the restoring force represented by the dashed curve in the figure, and the other is the force due to the local trapping represented by the deviation of the loop from the curve. The curve gives the intensity of the restoring force divided by $2P_0$ as a function of the wall position, since the field E exerts a force $2P_0E$ per unit area of the wall.

The restoring force may be imputed to the internal stresses; the hysteresis loop proves that the principal factor determining the domain structure is the internal stress. The local trapping may be the cause of the Barkhausen effect, but the observed region in which the wall propagates in one step ($5\times10^{-6}-1\times10^{-4}$ cm^3) is very large compared with the Barkhausen region

estimated from conductivity pulses (several 10^{-8} cm^3).[5] Hence, each observed step of the propagation appears to consist of many discontinuous processes.

The propagation of the wall is sometimes so sluggish that it takes several seconds to reach a new equilibrium position (Fig. 11, dashed lines). This behavior seems to be related to the fatigue effect described in Sec. VII.

For small voltages, the displacement of the wall cannot be observed, but a few of the wedge-shaped domains are comparatively sensitive and move smoothly in weak fields. The smallest field for which their expansion and contraction were confirmed is 4 v/cm at 13°C. Hence some wedge-shaped domains can contribute to the static initial dielectric constant, i.e., the

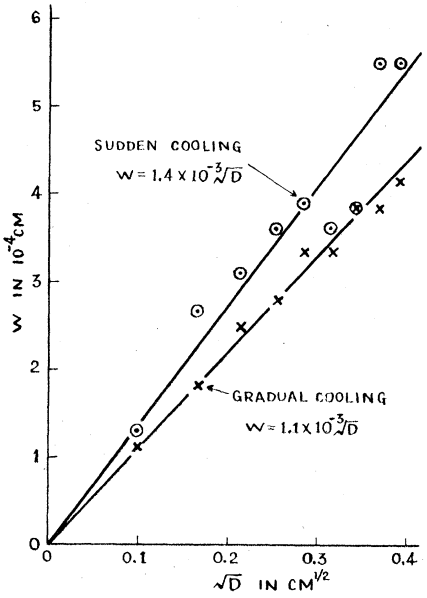

FIG. 10. Examples of proportionality between domain width W and square root of thickness D. The sample was kept at 45°C for 15 hours and then cooled. The points × represent cooling from 45°C to 13°C; the points ⊙ represent gradual cooling from 45°C to 24°C and sudden cooling from 24°C to 13.5°C.

dielectric constant for the static field smaller than the critical field called "sprung feld" by Kurtschatow.[6]

When the field is removed and the crystal turns from a single domain to multidomain, the growing of a domain starts with a fusiform or wedge shape.

VI. PROPAGATION VELOCITY OF THE DOMAIN WALL

The motion of the wall was studied by means of an apparatus consisting of a sector and a generator of square-wave voltage (Fig. 12). The generator is an ebonite disk to which copper bands A, B, and C are attached on one side, and A', B', and C' on the opposite side; C is connected to A' and B, while C' is connected

[5] S. Kojima and K. Kato, J. Phys. Soc. Japan **5**, 379 (1950).
[6] B. Kurtschatow and I. Kurtschatow, Physik Z. Sowjetunion **3**, 321 (1933).

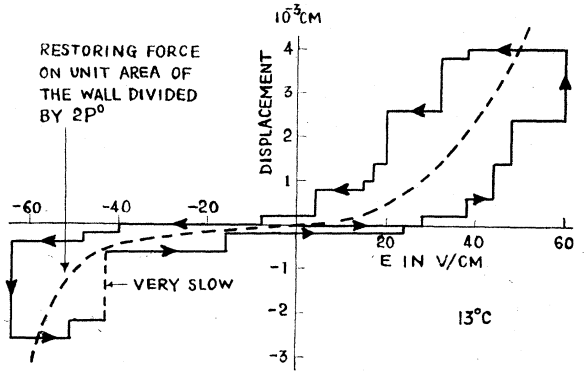

FIG. 11. Wall displacement by the effect of the electric field.

to A and B'. When a static voltage is applied between C and C' of the rotating disk, a square-wave voltage is produced from the brushes in contact with the outside copper bands. The sector rotates with the generator while the crystal is held stationary. The crystal is viewed through a window in the sector by means of a microscope. If the motion of the wall is the same during each cycle of the applied square-wave voltage, the wall will appear to be stationary. The time delay between the start of the square-wave cycle and the observation of the wall can be varied by changing the initial setting of the window relative to the contacts. The actual motion of the wall was not stationary enough so that the wall could always be observed at the same position, but there was a position at which the wall appeared most frequently. These positions, plotted in Fig. 13, show that the internal restoring force on the wall makes the propagation velocity larger as the wall approaches its original position and smaller as it recedes. The propagation velocity near the original position of the wall is in general a linear function of the field (Fig. 14). The wedge-shaped domains have no specific propagation velocity.

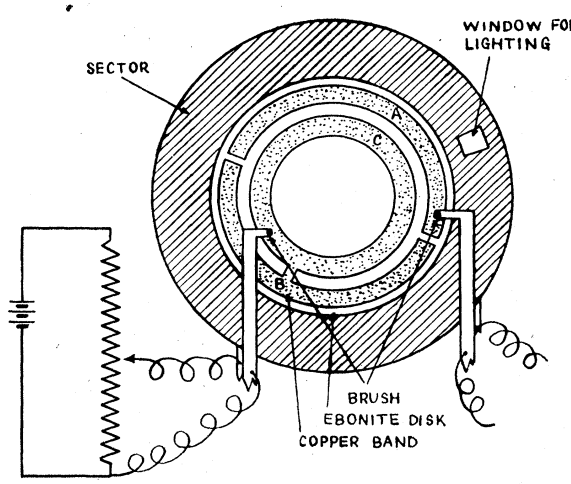

FIG. 12. Apparatus to study the motion of the wall for square wave voltage.

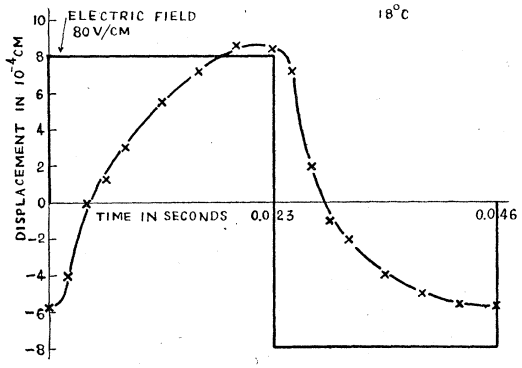

FIG. 13. Motion of the wall at 22 cps.

VII. FATIGUE EFFECT

Dielectric fatigue consists in a reduction in the discharge after prolonged application of a field. Our ballistic measurement proved that the crystal is not fatigued above 24°C. This fact suggests that the fatigue of the crystal is related to the domain structure. The restoring force acting on a domain wall can be measured by observing the displacement of the wall as the field is increased and then decreased gradually (Fig. 11). We traced out in succession five hysteresis loops corresponding to the upper half of the loop in Fig. 11. The application of the positive field in tracing the first loop may leave a fatigued crystal for the second observation, which in turn may leave a more fatigued crystal for the third, and so on. Figure 15 proves that this is the case. It took about five minutes to complete one loop.

VIII. EFFECT OF STRESS Y_Z

A set of domains narrows and the other widens when a stress Y_z is applied. The crystal turns into a single domain crystal for strong Y_z, and its application for several minutes leaves a remanent state, which disappears when the crystal is warmed above the Curie temperature and cooled again.

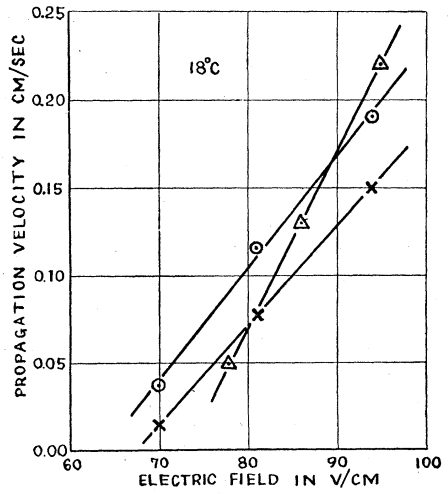

FIG. 14. Propagation velocity of the wall as a function of the electric field. The same marks are concerned with the same wall.

IX. ARTIFICIAL CREATION OF DOMAINS

A group of the *b* domains can be created artificially in the following way. Aluminum foil electrodes are attached to opposite faces of the crystal such that one half of each face was covered by the foil. The edges of the foil are made parallel to the *b* axis, and the part adjacent to the edges is observed (Fig. 16(a)). When the electric field is applied, inversion of the domains propagates from the electrode with a linear front parallel to the *b* axis (b). But the front breaks up as it goes far from the electrodes, while the original domains persist as wedges (c). The field is inverted (d) and then, if the field is inverted again before the linear front breaks up, the front remains and a new front propagates (e). The field is inverted again before the two fronts coalesce. Repetition of such operations leaves a group of *b* domains (f).

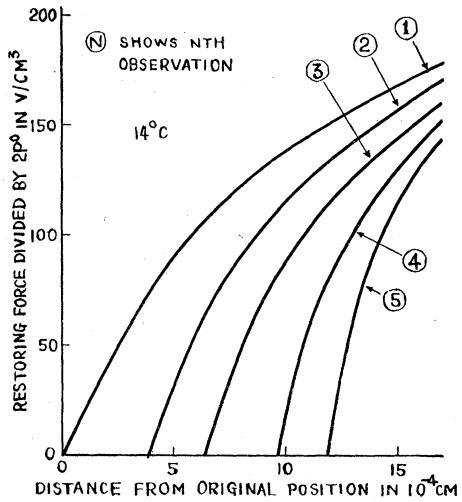

FIG. 15. Variation of the restoring force on unit area of the wall by prolonged application of the field.

The propagation of the inversion of the polarization out of the electrodes may be attributed to the conductivity of the crystal surfaces as suggested by S. Miyake. The inversion propagates through the whole crystal very rapidly if one breathes upon the specimen. The stable domains can be created only at low temperature and at a moderate dryness of the crystal surfaces. The *b* domains disappear and are replaced by the *c* domains if we warm the specimen above the Curie point and cool it again.

X. DOMAIN STRUCTURE OF KH_2PO_4

Inspection between crossed Nicols reveals that when *Z*-cut specimens of KH_2PO_4 are cooled below the Curie temperature they divide into many regions bounded by bright lines (Fig. 17). In general, the regions are several

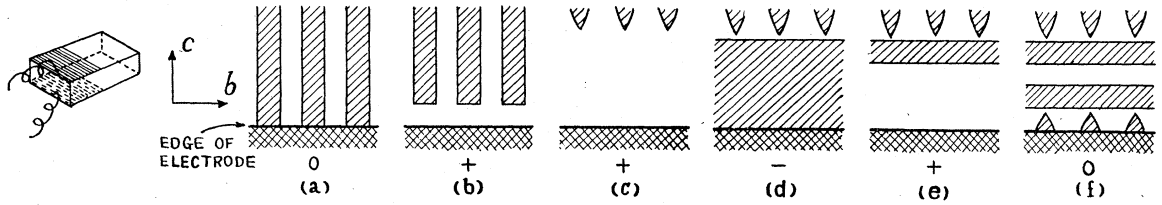

FIG. 16. Method for creating b domains.

tenths of a mm in width and several mm in length; some of these regions are further divided into many fine regions of a width of several hundredths of a mm (the white part in Fig. 17). The boundaries are parallel to the a axis. Most of them can be observed without the upper Nicol and look like minute cracks. These boundaries correspond to the possible domain boundaries or twin planes of KH_2PO_4, which are the (100) and (010) planes, as has been pointed out by H. Takahashi.[7] But we have not found any difference between extinction positions or any signs of double refraction or differences in the absorption coefficients of neighboring domains as discussed in Sec. II.

We have not found any change of the structure at the Curie point in X-cut specimens. When Z-cut specimens are observed between crossed Nicols and cooled beyond the Curie point, a slightly dark region propagates in the crystal with a distinct front. Its velocity is about 2 cm/sec. Just behind the front the boundaries suddenly appear in succession. This propagation may correspond to the phase transition, and the above facts prove that, in general, the phase transition in KH_2PO_4 propagates from only one nucleus. When the temperature is increased a few of the boundaries suddenly disappear before the whole crystal recovers its original structure.

XI. DOMAIN STRUCTURE OF MINIMUM ENERGY

It is the purpose of this section to determine the domain structure which will minimize the internal energy of rochelle salt if the contributions of the electrostatic energy to the internal energy are taken into account. As a first approach to the problem, it was assumed that the difference between the x component of the polarization and the saturation polarization is directly proportional to the field strength E_x. This relation is expressed by the equation

$$\epsilon_a E_x = 4\pi(P_x - P_0), \tag{1}$$

where ϵ_a is the initial dielectric constant in the X direction and P_x is the component of the polarization in the X direction. The problem of determining the domain structure which will minimize the free energy is then analogous to that of a ferromagnetic film with very large anisotropy.[8]

Suppose that at the time $t=0$ the crystal polarizes spontaneously and a periodic domain structure with domain width W results (Fig. 18). The electrostatic potential ψ must satisfy the following equations: in air ($x>0$)

$$\nabla^2\psi = 0;$$

in the crystal ($x<0$)

$$\epsilon_a(\partial^2\psi/\partial x^2) + \epsilon_b(\partial^2\psi/\partial y^2) = -4\pi\int_0^t [\sigma_a(\partial^2\psi/\partial x^2) + \sigma_b(\partial^2\psi/\partial y^2)]dt.$$

The following boundary conditions must be satisfied at the surface ($x=0$):

$$4\pi P_0(y) - \epsilon_a(\partial\psi/\partial x)_{x=-0} + (\partial\psi/\partial x)_{x=+0} = 4\pi\int_0^t \sigma_a(\partial\psi/\partial x)_{x=-0}dt;$$

and

$$(\partial\psi/\partial y)_{x=-0} = (\partial\psi/\partial y)_{x=+0}.$$

Here ϵ_b is the dielectric constant along the b axis, σ_a and σ_b are the conductivities along the a and b axes, respectively, and $P_0(y)$ is the saturation polarization of the domains. The solution of these equations at $t=0$ gives the following expression for the electrostatic energy F_{es} per unit area of the surface at $t=0$:

$$F_{es} = 1.7P_0^2W/[1+(\epsilon_a\epsilon_b)^{\frac{1}{2}}],$$

using

$$F_{es} = \frac{1}{8\pi}\int \mathbf{E}(\mathbf{D} - 4\pi\mathbf{P}_0(y))dxdy,$$

where $\mathbf{E}$ is the electric field, $\mathbf{D}$ is the electric displacement, and $\mathbf{P}_0(y)$ is the saturation polarization expressed as vector quantities. As described in Sec. IV, the domain width in an actual crystal is much smaller than its thickness (corresponding to a crystal thickness of

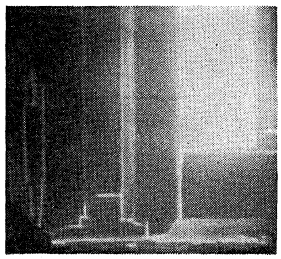

FIG. 17. Z-cut specimen of KH_2PO_4 observed between crossed Nicols below the Curie point (×11).

[7] H. Takahashi, Kagaku **20**, 495 (1950).
[8] C. Kittel, Phys. Rev. **70**, 965 (1946).

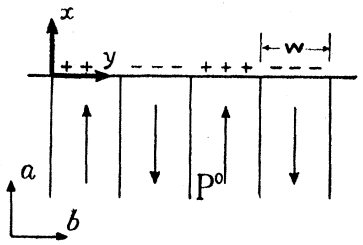

FIG. 18. Domain structure of period $2W$.

10^{-2} cm the domain width is only about 10^{-4} cm), so that the electrostatic energy F_e of a specimen may practically be taken as twice F_{es};

$$F_e=3.4P_0^2W/(\epsilon_a\epsilon_b)^{\frac{1}{2}},$$

with $(\epsilon_a\epsilon_b)^{\frac{1}{2}}\gg 1$. On the other hand, there is the surface energy F_w of the domain boundaries, and if this energy per unit area is denoted by γ, it is $F_w=\gamma D/W$. Therefore the domain width which makes $F=F_e+F_w$ a minimum is

$$W=0.54[(\epsilon_a\epsilon_b)^{\frac{1}{2}}\gamma D]^{\frac{1}{2}}/P_0. \tag{2}$$

Thus W is proportional to the square root of D. Some time after the domain structure has formed, F_e can be expressed by

$$F_e=3.4P_0^2W(\epsilon_a\epsilon_b)^{\frac{1}{2}}/(\epsilon_a+4\pi\sigma_a t)(\epsilon_b+4\pi\sigma_b t).$$

The rate of decay of F_e with time depends principally on σ_b, since ϵ_a is much larger than ϵ_b. Assuming the validity of the above equation for F_e and the equality of σ_b with σ_a, and taking $\epsilon_b=9.8$ esu and, according to Valasek,[9] $\sigma_a=0.1$ esu, F_e is found to decay to one-half of its original value in 8 sec.

If σ_b is much smaller than the above value and the crystal is cooled very rapidly below the Curie point, the domain structure of the crystal may be formed at a temperature somewhat lower than the Curie temperature, and the values of ϵ_a, γ, and P_0 at that temperature may determine the relation between W and D. We may thus explain the effect of sudden cooling shown in Fig. 10.

XII. THEORY OF THE DOMAIN WALL OF ROCHELLE SALT

The purpose of this section is to find expressions for the domain wall energy and the wall thickness. It is assumed that the crystal is a semi-infinite slab and contains only domains perpendicular to the b axis, and that the polarization $P(y)$ is a continuous function of y. According to Mueller, the free energy A per unit volume of the crystal with polarization P is given by

$$A=aP^2+bP^4, \tag{3}$$

where a is one-half of the reciprocal susceptibility for zero polarization and has a negative value in the ferroelectric region, and b is one-fourth of Mueller's B, which is a positive function of the temperature. Hence, the free energy increases due to the existence of the wall by

$$\gamma_1=\int_{-\infty}^{+\infty}[(aP(y)^2+bP(y)^4)-(aP_0^2+bP_0^4)]dy$$

per unit area of the wall. Equation (3) gives us also the expression for P_0 which makes A a minimum; $P_0^2=-a/2b$, so that γ_1 can be written as

$$\gamma_1=\int_{-\infty}^{+\infty}b(P_0^2-P(y)^2)^2dy. \tag{4}$$

The electric field along the X direction is given by $(\partial A/\partial P)_T$. From Eq. (1) the dielectric constant ϵ_a can then be expressed in terms of P_0 and b.

$$\epsilon_a=\pi/(2bP_0^2). \tag{5}$$

Of all the contributions to the free energy of the crystal caused by the polarization, only those are contained in γ_1 which may be determined from the polarization at each point along the crystal surface alone. The contributions of the entropy terms of the dipoles (such as the 1–10 hydrogen points[10]) has therefore already been taken into account in γ_1. However, the contributions to free energy arising from the dipole-dipole interactions and the lattice deformations must also be considered. These will involve terms which are not already contained in γ_1, since γ_1 neglects those contributions to the free energy of the crystal which depend on the fact that the polarization $P(y)$ differs from point to point along the crystal surface. The energy $A_{d,i}$ of the interaction between the dipole μ_i and the field caused by all the other dipoles μ_j's is given by

$$A_{d,i}=-\mu_i\textstyle\sum_j\alpha_{ij}\mu_j=-\beta_iP(y_i)\sum_j\alpha_{ij}\beta_jP(y_j),$$

where α_{ij} is determined by the distance and the angle between the dipoles μ_i and μ_j, and β_i is the constant of proportionality between $P(y_i)$ and μ_i, (i.e., $\mu_i=\beta_iP(y_i)$). If an imaginary sphere of sufficiently large radius is drawn around μ_i, the summation may be replaced by an integration outside this sphere. We now approximate $P(y)$ by the first four terms of a Taylor series expansion, assuming that even for the relatively small radius around μ_i for which this expansion is a valid approximation, the replacement of the summation by an integration will not produce an excessively large error. $A_{d,i}$ then becomes

$$A_{d,i}=-\beta_iP(y_i)[f_{0i}P(y_i)+f_{1i}P'(y_i)+f_{2i}P''(y_i)+f_{3i}P'''(y_1)],$$

where the f_{ki}'s are constants depending on the arrangement of the dipoles. The first term in this expression for $A_{d,i}$ corresponds to the interaction energy when the whole crystal is uniformly polarized with a polarization

[9] J. Valasek, Phys. Rev. **20**, 639 (1922).

[10] W. P. Mason, Phys. Rev. **72**, 854 (1947).

$P(y_i)$ and this is already contained in γ_1. Therefore, the increase of the interaction energy due to the fact that the polarization at positions other than at y_i differs from $P(y_i)$ is expressed by the sum of the other three terms. In order to obtain that part of the interaction energy of the dipoles which is not already contained in γ_1, each of the last three terms in the above expression for $A_{d,i}$ must be summed over all i's and the result divided by two. In order to compute the energy, these summations are replaced by integrations over all space and, since $P(y)P'(y)$ and $P(y)P'''(y)$ are odd functions of y, their integrals vanish. Only the term containing $P(y)P''(y)$ will therefore contribute to the wall energy. Hence

$$\gamma_2=-\int_{-\infty}^{+\infty} fP(y)P''(y)dy, \tag{6}$$

where f is a function of β_i, f_{2i}, and the volume of the unit cell. Here we assume that f is positive, since this assumption leads to agreement with the experimental results.

The spontaneous polarization of rochelle salt is directly accompanied by a shear strain y_z and also by the strains x_x, y_y, z_z. These strains at the position y in the wall may be set up as if the whole crystal were uniformly polarized with the polarization at y, and thus the energy due to these lattice deformations is contained in γ_1, unless the strains cause mismatch between adjacent Z-X planes. The energy due to the strains y_z and y_y is therefore already contained in γ_1, since these strains represent a slip and a displacement between adjacent Z-X planes, respectively. But the x_x and z_z strains must deviate from their original values, since they are deformations of a Z-X plane itself. According to Mueller, they are related to P by $x_x=\varphi_1P^2$ and $z_z=\varphi_3P^2$, where φ_1 and φ_3 are constants. As to x_x, φ_1 is negative and thus the larger the value of P is, the more the crystal contracts along the X direction. Therefore, the crystal must be thicker at the wall than the other parts, if the above relation holds also in the wall. But this change of thickness cannot be set up in the crystal of which the dimensions are infinite, as assumed at the beginning of this section. Therefore, the additional strains $\varphi_1(P_0^2-P(y)^2)$ and $\varphi_3(P_0^2-P(y)^2)$ must be set up in the wall to avoid the deformations, and thus the elastic energy per unit area of the wall is given by

$$\gamma_3=\int_{-\infty}^{+\infty} g(P_0^2-P(y)^2)^2dy. \tag{7}$$

Here

$$g=\tfrac{1}{2}(c_{11}\varphi_1^2+c_{33}\varphi_3^2), \tag{8}$$

where c_{11} and c_{33} are elastic stiffness coefficients.

The domain wall energy γ is obtained by adding γ_1, γ_2, and γ_3 expressed by Eqs. (4), (6), and (7); thence

$$\gamma=\int_{-\infty}^{+\infty}[(b+g)(P_0^2-P(y)^2)^2-fP(y)P''(y)]dy. \tag{9}$$

In order to determine $P(y)$ we now have to minimize γ, and therefore the variation of the integral with respect to $P(y)$ must be equated to zero. Hence $P(y)$ must satisfy the following equation:

$$2(b+g)(P_0^2-P(y)^2)P(y)-fP''(y)=0.$$

The solution is

$$P(y)=P_0\tanh(2y/T), \tag{10}$$

where T is the thickness of the domain wall and is given by

$$T=2f^{\frac{1}{2}}/[(b+g)^{\frac{1}{2}}P_0]. \tag{11}$$

From Eqs. (9), (10), and (11), we obtain

$$\gamma=\tfrac{8}{3}[f(b+g)]^{\frac{1}{2}}P_0^3. \tag{12}$$

Using Eqs. (5) and (12), we can write Eq. (2) as

$$W^2/D=1.0[\epsilon_b f(b+g)/b]^{\frac{1}{2}}.$$

Here $f(b+g)$ is almost temperature independent, since f and g will not depend much on temperature and the constant b ($\sim 2\times10^{-8}$ at 20°C) is very small compared with g($>3\times10^{-7}$), though it varies with temperature. The value of ϵ_b increases slightly with temperature but its variation is small compared with the increase of b. Therefore W^2/D may decrease with increasing temperature and may also have a finite value at the Curie point. The experimental values are in general agreement with these results though the decrease of the experimental value of W^2/D with temperature (which is proportional to $1-0.03\theta$, where θ is the temperature in degrees centigrade[11]) is steeper than that of $1/b^{\frac{1}{2}}$ ($\alpha 1-0.01\theta$).[12] Using the values at 24°C; $W^2/D=1.2\times10^{-6}$, $\epsilon_b=9.8$, and $b=2.0\times10^{-8}$, we have

$$[f(b+g)]^{\frac{1}{2}}=5.4\times10^{-11}, \tag{13}$$

and thus Eq. (12) becomes

$$\gamma=1.4\times10^{-10}P_0^3.$$

The value of P_0 at 0°C is 740 esu (its maximum value) and at 20°C it is 420 esu, so that $\gamma=0.057$ erg/cm^2 at 0°C and $\gamma=0.010$ erg/cm^2 at 20°C.

It was impossible to evaluate g exactly since we could not find any measured value of φ_3; however, assuming $c_{33}\varphi_3^2=c_{11}\varphi_1^2$ and using[13] $c_{11}=4.0\times10^{11}$ and $\varphi_1=-1.2\times10^{-9}$, we obtain $g=5.8\times10^{-7}$ from Eq. (8), and thus $f=4.9\times10^{-15}$ from Eq. (13). Using these values, Eq. (11) can be written as

$$T=1.8\times10^{-4}/P_0.$$

Thus $T=24$A at 0°C, and $T=43$A at 20°C. These walls are therefore much thinner than the ferromagnetic domain walls ($\sim10^3$A).

In conclusion it may be stated that the variation of

[11] From the data in Fig. 10, assuming that $W=1.4\times10^{-3}D^{\frac{1}{2}}$ at 14°C.
[12] Reference 1, p. 627, Fig. 146.
[13] See reference 1, p. 122.

the polarization in the wall is determined by two factors: the elastic energy which tends to decrease the wall thickness, and the dipole interaction energy which is greatly increased by steep changes in P, since PP'' must be negative in the wall, and which therefore tends to increase the width of the wall.

The authors wish to thank Dr. A. von Hippel for his kindness in introducing their manuscript to the editors of *The Physical Review*. They also wish to express their gratitude to Dr. H. Kawai and Mr. M. Marutake for supplying many rochelle salt crystals, and to Dr. E. Kanda for his suggestion on design of the microscope stage for low temperature. They also are indebted to Mr. Y. Katsui for his valuable help at the beginning of this work, and to Mr. I. Ohmura and Mr. N. Nishida for their valuable help.

PHYSICAL REVIEW VOLUME 90, NUMBER 2 APRIL 15, 1953

The Infrared Absorption Characteristics of Thermiated Germanium*

D. H. RANK AND D. C. CRONEMEYER
General Electric Company, Electronics Laboratory, Syracuse, New York
(Received December 18, 1952)

The infrared absorption spectrum of thermiated germanium has been obtained. It is shown that this material in addition to its greatly changed electrical properties becomes strongly absorbing in the infrared. A 48-hour anneal in air at 500°C restores the infrared transmission to that identical with the untreated control sample. The absorption spectrum for chemically P-doped germanium has been obtained and the absorption cross section for the P-doped material compared with that of thermium.

IT is well known that thermal treatment and subsequent quenching of germanium produces the appearance of acceptor centers. The radically different electrical properties of heat-treated samples which have been quenched has resulted in the common application of the name "thermium" to germanium semiconductors which have been thus thermally processed.

We have investigated the infrared transmission of thermiated germanium and also examined the effect of annealing upon the absorption spectrum of a thermiated sample.

The study of thermium was undertaken in the following manner: A 5-ohm-cm homogeneous N type single crystal was sectioned into four pieces each 1 cm thick. The specimens were given treatments as follows:

(a) Control (5-ohm-cm N type).

(b) Light thermal shock (700°C quenched into air 5-ohm-cm N→8-ohm-cm N).

(c) Strong thermal shock (900°C quenched into air 5-ohm-cm N→1.55-ohm-cm P).

(d) Strong thermal shock (900°C quenched into air plus 48-hour anneal of 500°C in air. 5-ohm-cm N→1.6-ohm-cm P→6–9-ohm-cm N).

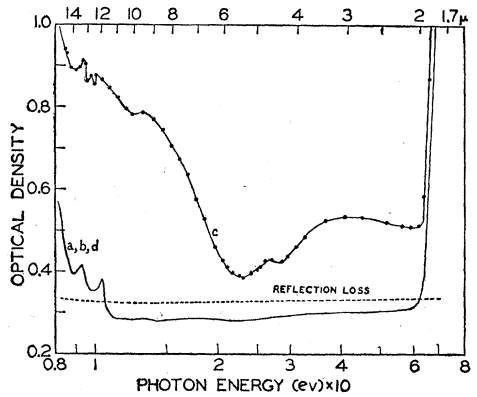

FIG. 1. Curve marked a, b, d represents the identical optical density *vs* wavelength curves obtained for germanium samples a, b, and d, respectively. Curve c represents the results obtained with the thermiated germanium sample c. The dotted curve was calculated from refractive index data.

The specimens described above were ground optically plane and parallel. A good optical polish was produced on the surfaces, care being taken to assure that the surface quality was sufficiently good so that surface defects could not influence the transmission measurements.

The infrared transmission of the germanium samples has been measured by the authors at the Pennsylvania State College and at the General Electric Electronics Laboratory, respectively. Both spectrophotometers were Perkin-Elmer model 112 double-pass high resolution instruments.

Briggs[1] has measured the index of refraction of bulk germanium in the 1.8- to 3-micron region making use of the method of minimum deviation. We have measured the index of refraction of bulk germanium in the 8–12 micron region by means of an interference method. A parallel plate of 0.5-mm thickness was used for this experiment, and the value obtained for the index of refraction was 3.96 ± 0.02, which is substantially in agreement with the value expected from an extrapola-

* This work was supported by the Air Materiel Command, the Bureau of Ships, and the U. S. Signal Corps.

[1] H. B. Briggs, Phys. Rev. **77**, 287 (1950).

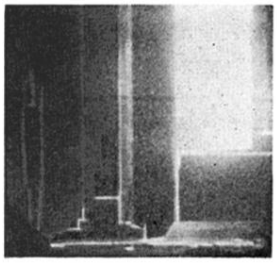

FIG. 17. *Z*-cut specimen of KH_2PO_4 observed between crossed Nicols below the Curie point ($\times 11$).

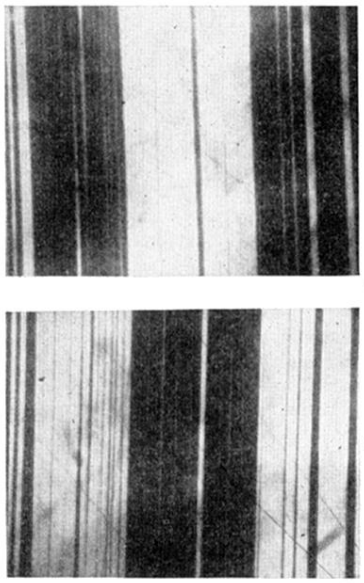

FIG. 3. *X*-cut specimen of rochelle salt observed between crossed Nicols (×50). The *c* axis is rotated from the plane of a Nicol (A) to the left; (B) to the right.

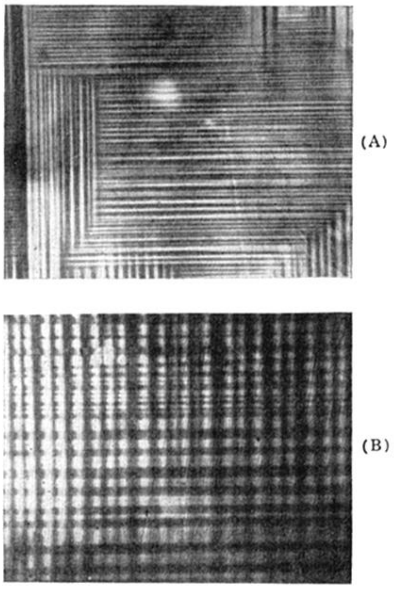

FIG. 4. Co-existence of *b* and *c* domains. (A) A group of fine *b* domains at the crystal surface (×80). (B) A specimen of which the upper half consists of *b* domains and the lower half *c* domains (×50).

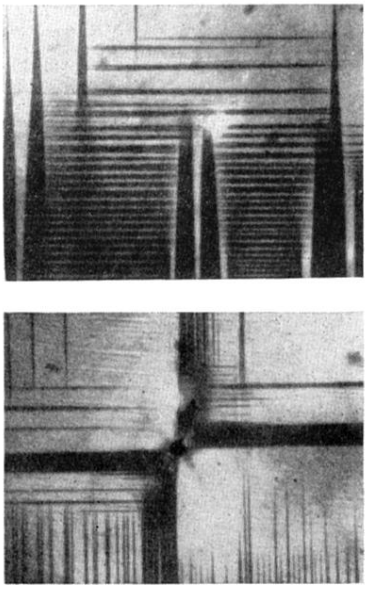

FIG. 5. Domain structure caused by strong internal stress (×80). The *b* and *c* directions are the same as in Fig. 4. (A) Peculiar co-existence of *b* and *c* domains. (B) Domain structure around a hole (black spot in the center).

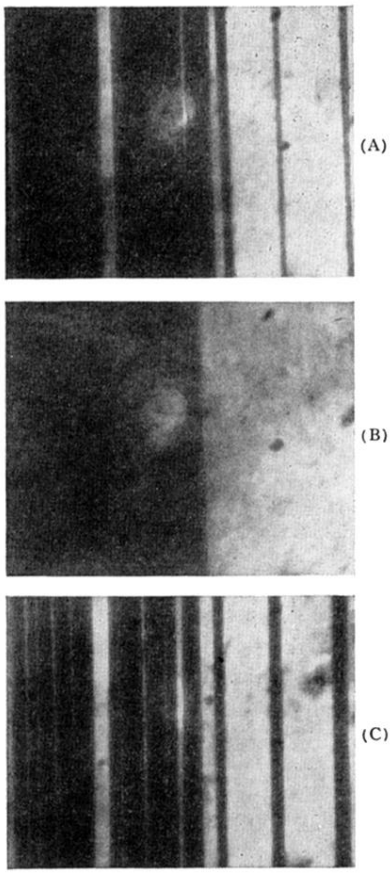

FIG. 6. Effect of temperature (×210). (A) 15°C. (B) 22°C. (C) 15°C after keeping at about 25°C for several minutes.